Research Article

# Pectin-*Aloe vera* Gel Biopolymer Transdermal Patches for Prospective Limonene Delivery System: Characterization and *in vitro* Release Kinetics

Nisaul Fadilah Dalimunthe*, Michael Michael, Thiodorus Marvin Tjandra, Iryuni Madinar Pulungan, Muhammad Thoriq Al Fath and Rivaldi Sidabutar
Department of Chemical Engineering, Faculty of Engineering, Universitas Sumatera Utara, Medan, Indonesia

Jeslyn Harsono
Department of Food Science and Biotechnology, College of Agriculture and Life Sciences, Kangwon National University, Chuncheon, South Korea

Pema Yangden
Department of Chemical Engineering, Faculty of Engineering in Foreign Languages, National University of Science and Technology POLITEHNICA Bucharest, Bucharest, Romania

Sang Kompiang Wirawan
Department of Chemical Engineering, Faculty of Engineering, Universitas Gadjah Mada, Yogyakarta, Indonesia

* Corresponding author. E-mail: nisaul.fadilah@usu.ac.id DOI: 10.14416/j.asep.2026.01.004
Received: 4 July 2025; Revised: 24 September 2025; Accepted: 5 November 2025; Published online: 12 January 2026


**Abstract**
Pectin-based transdermal systems suffer from inadequate mechanical properties and rapid biodegradation, limiting pharmaceutical applications. This study addresses these critical limitations through novel transdermal patches fabricated with varied pectin concentrations (7–11g) and *Aloe vera* (AV) gel extract (0–10% w/w) as a bioactive matrix for *Citrus aurantifolia*-derived limonene delivery. Patches were fabricated via solvent casting using pectin and AV gel, followed by characterization of physicochemical properties (swelling, moisture content, and biodegradation), surface morphology (SEM), and molecular interactions (FTIR). Mechanical properties were assessed by tensile testing and *in vitro* release studies were performed using a Franz diffusion cell with benzoylated dialysis membrane to evaluate release kinetics. Optimal formulations demonstrated a remarkable 7.39-fold tensile strength enhancement (6.070 ± 0.008 MPa), superior *in vitro* release kinetics, with 57.85 ± 0.60% initial burst release, and 94.61 ± 0.30% sustained delivery over 120 h. Korsmeyer-Peppas kinetics (n = 0.472) confirmed non-Fickian diffusion mechanisms. Economic viability was established (production cost: 2.5 USD/L; net profit: 2.8 USD/L), presenting a commercially feasible and biodegradable solution for pharmaceutical applications. Future investigations will focus on *in vivo* evaluation to confirm the efficacy, safety, and clinical applicability of the developed patches.

**Keywords**: *Aloe vera*, Biopolymer, Limonene incorporation, Pectin, Transdermal drug delivery

## 1 Introduction

The development of efficient drug delivery systems remains a significant priority in pharmaceutical research, with transdermal patches emerging as a promising method for controlled and non-invasive administration of therapeutic compounds. Transdermal drug delivery has drawn a lot of attention for the past decades due to its advantages over conventional drug delivery methods. These advantages include simplicity, ease of handling, precise dose control, patient self-administration, and relatively simple storage requirements

compared to other drug delivery systems [1]. The primary objective in the formulation of transdermal drug delivery systems is to optimize the percutaneous flux while simultaneously minimizing the retention and metabolic degradation of the active pharmaceutical compounds [2].

As illustrated in Figure 1, transdermal drug delivery systems specifically utilize noninvasive administration techniques that cause minimal pain and burden to patients, enabling safe and convenient administration to pediatric or geriatric populations [3], [4]. The transdermal drug delivery mechanism operates through sequential phases: Application of the drug-containing patch or formulation to the skin surface, drug release from the formulation, penetration across the stratum corneum, permeation through epidermal and dermal layers, absorption into cutaneous microcirculation, and ultimately entry into systemic circulation [5], [6]. The TDDS offers painless drug administration with multiple advantages over conventional oral and injectable methods, including circumvention of first-pass metabolism, enhanced bioavailability, improved patient adherence, decreased dosing frequency, sustained and controlled drug release, superior drug stability, and avoidance of systemic toxicity, particularly gastrointestinal irritation [7].

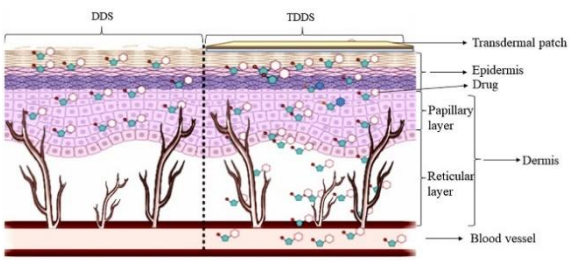


**Figure 1**: Schematic representation of a conventional drug delivery system (DDS) and a transdermal drug delivery system (TDDS), illustrating drug transport across skin layers.

The polymeric film within transdermal patches comprises three essential components: polymer, plasticizer, and penetration enhancer. Various polymers may be incorporated into the film, including polyvinyl alcohol, hydroxypropyl methacrylate, pectin, or polyvinyl pyrrolidone [8]. Among these candidates, pectin emerges as an exceptionally promising biopolymer for transdermal patch fabrication. This natural polysaccharide, chemically composed of galacturonic acid and abundantly present in ripe fruits, offers numerous advantages. It finds extensive application across pharmaceutical, cosmetic, food, and biological sectors owing to its cost-effectiveness, biocompatibility, biodegradability, and non-toxicity [9], [10]. Complementing the polymer, plasticizers may be incorporated to enhance patch stability and flexibility by reducing intermolecular forces and facilitating polymer chain mobility [11]. Glycerol represents one of the most commonly employed plasticizers in polymer film production. Within transdermal formulations, appropriate penetration enhancer excipients are vital, as they can modify bioavailability and drug penetration [12].

A study by Asfaw *et al*., [13] demonstrated that incorporating citron peel pectin into edible films generally enhances their mechanical properties. Improvements in tensile strength (4.00–7.00 MPa), elastic modulus (607.01–690.12 kg/cm), and elongation at break (22.21–29.5%) were observed with increasing pectin content. Similarly, a study by Nisar *et al*., [14] reported favorable mechanical characteristics when pectin was combined with young apple polyphenols in film formulation. These studies supported the potential of pectin to strengthen and improve the overall performance of biopolymer films, making it a promising candidate for various applications, including transdermal patches.

*Aloe vera* (AV) contains lignin that has been shown to enhance drug penetration. This natural enhancement is attributed to lignin's ability to interact and temporarily alter the structure of the stratum corneum, facilitating the passage of drug molecules through the skin barrier. Additionally, AV contains saponins, which act as a natural cleansing agent, potentially increasing the skin's reception to topical treatments [15], [16]. The combination of these properties makes AV multifunctional ingredient in transdermal patch formulations, potentially improving both drug delivery efficiency and overall patch performance.

Studies on AV as a penetration enhancer in drug delivery systems have yielded promising results. Bhutkar *et al*., [17] investigated the effect of AV on lidocaine delivery and discovered that at a 3% concentration, AV, as a natural enhancer, was able to increase lidocaine penetration by 79.18%. Another study conducted by Sainy *et al*., [18] shows that the formulation of AV–based emulgel with 20% of AV incorporation exhibits desoximetasone permeation of 95.40 ± 1.6% over a 7–hour period using a Franz diffusion cell. These findings strongly suggest that the introduction of AV as a natural penetration enhancer

in transdermal formulations could significantly improve drug permeation across the skin barrier. Limonene, a cyclic terpene prevalent in citrus essential oils, is extensively acknowledged as a safe flavoring agent in diverse food products and a prevalent fragrance constituent in cosmetics [19]. Beyond its aromatic properties, studies have demonstrated that limonene can diminish collagenase and elastase enzymatic activities, suppress melanogenesis, and combat *Cutibacterium acnes*, indicating its potential efficacy in addressing multiple dermatological concerns, including senescence, irregular pigmentation, and acne [20]. However, despite the established individual mechanisms of both AV and limonene, their combined effects in transdermal systems remain largely unexplored, representing a significant research gap in understanding potential interactive enhancement mechanisms.

The objective of this study is to develop a pectin–AV transdermal patch incorporated with limonene and investigate the physicochemical and mechanical characteristics of the resulting formulation. The obtained transdermal patch was evaluated through *in vitro* release, skin penetration and retention studies using a modified Franz diffusion cell. The *in vitro* skin penetration study was performed in order to determine the possible transdermal penetration potential of the patch. This study presents a novel application of pectin as the primary polymer matrix for a limonene-loaded transdermal patch. Moreover, this study explores the innovative combination of limonene as the primary active ingredient alongside AV, aiming to uncover potential synergistic effects in transdermal delivery. This unique pairing may enhance the overall efficacy of the patch, leveraging limonene's therapeutic properties and AV's penetration-enhancing capabilities to create a more potent and efficient drug delivery system.

## 2 Materials and Methods

### 2.1 *Materials*

The requisite materials for this investigation were obtained as follows. Technical grade, low methoxyl pectin (degree of esterification <50%, molecular weight ~60,000–130,000 Da) was procured from Phy Edumedia (Malang, Indonesia). *Aloe vera* (AV) leaf and lime fruit (*Citrus aurantifolia*) were acquired from a local commercial market. Glycerol ($C_3H_8O_3$, 99.5% purity, molecular weight 92.09 g/mol, viscosity 1.412 Pa·s at 20 °C) and tween-80 (polyoxyethylene sorbitan monooleate, ≥95% purity, molecular weight ~1,310 g/mol, HLB value 15.0, critical micelle concentration 0.01% w/v) were purchased from Merck KGaA (Darmstadt, Germany). Distilled water (aquadest, $H_2O$, pH 6.8–7.2) was graciously supplied by the Laboratory of Food and Bioprocess Engineering at Universitas Gadjah Mada in Yogyakarta, Indonesia.

### 2.2 *Methods*

#### *2.2.1 Fabrication of pectin–AV transdermal patch*

The fabrication of the pectin–AV transdermal patch was conducted in two stages. In the initial stage, the AV leaf was rinsed and trimmed into a 1-inch size, then subjected to an hour–long aqueous immersion to remove the aloin compound. The green external cortex layer was removed and the transparent gel matrix was extracted using a spoon. The extracted gel, containing ~98–99% water with ~0.5–1.0% polysaccharides (predominantly acemannan), along with minor proteins, amino acids, phenolic compounds, lignin, and saponins [16], was crushed in a blender followed by filtration to eliminate contaminants. To stabilize the gel, a few drops of lime juice were added to adjust the pH to ~4.5–5.0 and to act as a natural preservative. The purified gel was subjected to heating at 60 °C for 30 minutes, subsequently combined with 1 mL of freshly expressed lime juice as a limonene source. The gel is formulated at variable concentrations of 0%, 4%, 6%, 8%, and 10% (v/v) [21], [22]. Following this, pectin at quantities of 7, 9, and 11 g was introduced into a beaker, followed by the addition of 100 mL of distilled water. This mixture undergoes thermal elevation to 80 °C with continuous agitation for 22 min. The solution was then permitted to cool to 45 °C, whereupon glycerin (2% of pectin mass) and the AV-lime extract composite were incorporated and homogenized through stirring. The resultant solution was transferred to a petri dish and desiccated in an oven at 80 °C for 2 h and allowed to cool under controlled ambient conditions (28 ± 2 °C, 50 ± 5% relative humidity) for 48 h before being carefully peeled off for further analysis [23].

#### *2.2.2 Characterization of pectin–AV transdermal patch*

Physicochemical and structural analyses were conducted to evaluate the properties and behavior of the pectin–AV transdermal patches. Water absorption, swelling ratio, and biodegradation tests were performed

to assess hydration, dimensional stability, and environmental decomposition. Scanning Electron Microscopy (SEM) and Fourier Transform Infrared Spectroscopy (FTIR) were employed to elucidate surface topography, internal structure, and chemical compositional profiles. All analytical examinations were executed in strict accordance with standardized protocols and validated methodological procedures.

The water absorption characteristics of pectin–AV biocomposite transdermal patches were investigated using ASTM D570–98 methodology [24]. While this standard was originally developed for plastics, its gravimetric principle has been successfully applied to similar hydrocolloid-based composite materials, including rice starch–tara gum-pectin films [25], demonstrating its validity for water-absorbing biocomposite systems. This protocol quantifies the rate of water absorption by immersing specimens entirely in distilled water maintained at 23 ± 1 °C for 24 hours. Sheet–shaped patch specimens (76.2 mm length × 25.4 mm width × 3.2 mm thickness) were fabricated, with initial dry mass measured and recorded. The test evaluates the percentage increase in specimen mass as a metric for water absorption capacity. To assess the patch's water absorption, specimens were extracted, with excess surface moisture removed using a lint–free cloth, and hydrated mass determined gravimetrically to the nearest 0.001 g immediately post–extraction. The differential mass between initial and hydrated states was utilized to calculate the water absorption percentage according to Equation (1).

$$\text{Water absorption (\%)} = \frac{M_t - M_0}{M_0} \times 100\% \quad (1)$$

Herein, $M_t$ represents the mass of the patches following water absorption at a specific time and $M_0$ signifies the initial mass of the dry specimens prior to immersion in distilled water.

The swelling ratio was determined utilizing simulated body fluid (SBF) at pH 7.4, in accordance with the methodology described by Jodati *et al*. [26]. Each patch specimen underwent precise gravimetric measurement ($M_1$) and subsequent immersion in SBF maintained at 36.5 ± 1.5 °C. At 20-minute interval, specimens were extracted, excess surface fluid was removed using filter paper, and the hydrated mass ($M_2$) was recorded until equilibrium conditions were established. The swelling ratio was quantitatively determined employing Equation (2) [27]:

$$\text{Swellling ratio (\%)} = \frac{M_2 - M_1}{M_1} \times 100\% \quad (2)$$

Herein, $M_2$ represents the mass of the swollen patch and $M_1$ denotes the initial dry mass of the patch specimen.

Biodegradation studies were conducted under in-situ soil burial conditions at the Universitas Sumatera Utara campus in Medan, Indonesia (latitude 3°33'43" N, longitude 98°39'23" E, altitude 33.41 m). The soil burial test was performed over a three-month period. Pectin–AV transdermal patches were prepared as 10 × 5 cm sheets, oven-dried at 60 °C for 2 h, and their initial masses recorded. Specimens were buried at a depth of 0.4 m in soil with 65–70% moisture content, at an ambient temperature of 32 ± 2 °C. The soil had a pH of 6.7 ± 0.2 and microbial activity consistent with an organic-rich substrate (total microbial count ~$10^6$ CFU $g^{-1}$, previously determined by plate count method). All buried patches were maintained without sunlight exposure. Soil hydration was maintained solely by precipitation and atmospheric humidity. After the third month, specimens were exhumed, cleaned with distilled water, and oven–dried to constant mass at 50 °C in an air oven [28]. The weight of patches after soil biodegradation tests was recorded. Each pectin–AV formulation was performed in triplicate to determine the mean mass loss. The percentage of biodegradation was calculated using Equation (3) [29]:

$$\text{Biodegradation (\%)} = \frac{M_4 - M_3}{M_3} \times 100\% \quad (3)$$

Herein, $M_4$ represents the mass of the patch after the soil biodegradation test and $M_3$ represents the original mass of the dry patch specimen.

Verification of the chemical composition and drug incorporation properties of the pectin–AV transdermal patches was conducted via FTIR spectroscopy (IRPrestige 21, Shimadzu Corporation, Kyoto, Japan). Morphological characterization of the fabricated transdermal patches was performed using Scanning Electron Microscopy (SEM) analysis – employing a type HITACHI TM3000 (Japan) instrument to provide high-resolution visualization of the surface of patches.

### *2.2.3 Mechanical properties of pectin-AV transdermal patch*

The mechanical properties of pectin–AV biocomposites were assessed using a Universal Testing Machine

(AGX–V2, Shimadzu Corporation, Kyoto, Japan) equipped with a 50 kN load cell. This multi-functional machine is capable of performing tensile, compression, bending, and creep testing with a reported accuracy of 0.5% when properly calibrated. The testing procedures adhered to ASTM D882–10 standards for thin–sheet materials [30]. Mechanical tests were conducted under controlled environmental (ambient temperature 28 ± 2 °C and 52 ± 5% relative humidity). Patch specimens were prepared with dimensions of 90 mm length × 20 mm width × 0.45 mm thickness. Elongation and breaking force were documented at the precise juncture of patch structural failure, with samples secured between two clamps in which the upper clamp applied tension at a rate of 5 mm/min [31]. Tensile strength (σ) was calculated via division of the maximum load by the original specimen cross-sectional area (Equation 4) and reported with three significant figures. Elongation at break (ε) was determined by dividing the extension at the moment of break by the initial length and multiplying by 100 (Equation 5), with resultant values expressed as percentages to two significant figures [30].

$$\text{Tensile strength (kPa)} = \frac{P_{max}}{A_0} \quad (4)$$

$$\text{Elongation at break (\%)} = \frac{\Delta L}{L_0} \times 100\% \quad (5)$$

Elastic modulus was ascertained by calculating the gradient of the initial linear segment of the load-extension curve, dividing the tensile stress by the corresponding strain at a designated point on this tangent. The elastic modulus was calculated using Equation (6) and reported to three significant figures.

$$\text{Elastic modulus (\%)} = \text{Slope} \times \frac{L_0}{A_0} \quad (6)$$

Herein, $P_{max}$ (in kPa) represents the breaking force, $A_0$ (in $mm^2$) denotes the cross–sectional area, $\Delta L$ (mm) signifies the sample deformation, and $L_0$ (mm) represents the initial sample length.

### *2.2.4 Drug release study of pectin–AV transdermal patch*

The pectin–AV patches underwent assessment of drug release capabilities via Franz diffusion cell methodology, with subsequent establishment of release kinetics. Benzoylated dialysis membrane served as the partition between donor and receptor compartments of the diffusion apparatus. The receptor medium consisted of phosphate buffer (pH 7.4) maintained at 37 ± 2 °C. A 1 $cm^2$ section of the pectin-AV film was situated within the donor compartment, while aliquots were withdrawn from the receptor compartment at predetermined intervals throughout a cumulative 120 h experimental period. The extracted samples underwent centrifugation at 3,000 rpm and the quantity of limonene released into the receptor fluid at respective time was quantified through spectrophotometric absorbance measurements (UV–1800, Shimadzu Corporation, Kyoto, Japan). The drug release kinetic profile was subsequently fitted to various mathematical models, including zero-order, first-order, and Korsmeyer–Peppas using Origin 2025 software (OriginLab Corporation, Massachusetts, USA). The optimal model for elucidating limonene release kinetics from the pectin–AV patch was selected based on the highest goodness of fit [32].

Benzoylated dialysis membrane was selected to evaluate formulation–controlled *in vitro* release of limonene from the pectin–AV matrix. The dialysis membrane provides a standardized permeability characteristic, reproducible pore structure, and absence of biological variability that would confound comparative analysis between formulations. While this synthetic membrane cannot replicate the complex stratum corneum barrier and selective permeability of human skin, it provides a controlled environment for evaluating in vitro release kinetics and formulation optimization. The membrane's molecular weight cutoff and porosity also allow for initial assessment of drug diffusion mechanisms prior to more physiologically relevant skin permeation studies.

### *2.2.5 Statistical analysis*

The attained experimental data, encompassing water absorption, swelling kinetics, biodegradation profiles, tensile strength parameters, elongation at break values, Young's modulus measurements, and *in vitro* drug release kinetics, were conducted in triplicate (n = 3), and the results are expressed as mean ± standard deviation (SD). Statistical analysis was performed utilizing two–way analysis of variance (ANOVA), with statistical significance established at a threshold of $p$–value < 0.05 (Origin 2025b, OriginLab Corp., Massachusetts, USA). Actual $p$–value obtained from the analysis are reported in the Results section rather than only threshold values. In addition to statistical significance ($p$–value < 0.05), the magnitude of change

between formulations is interpreted in the context of potential biological relevance.

## 3 Result and Discussion

### 3.1 *Characteristic of pectin-AV transdermal patch*

#### *3.1.1 Water absorption*

Water absorption of the pectin–AV transdermal patch was evaluated to determine its hydrophilic properties. Figure 2 represents the results of this assessment. The incorporation of AV into the pectin polymer matrix enhances the water absorption ability of the patch significantly. The highest water absorption of the patch was recorded at 11 g of pectin and 10% AV, reaching the water absorption of 42.136 ± 0.249%. This presents a substantial increase ($p$–value = 0.032, n = 3) from the 15.690 ± 0.050% water absorption observed in the pristine pectin patch.

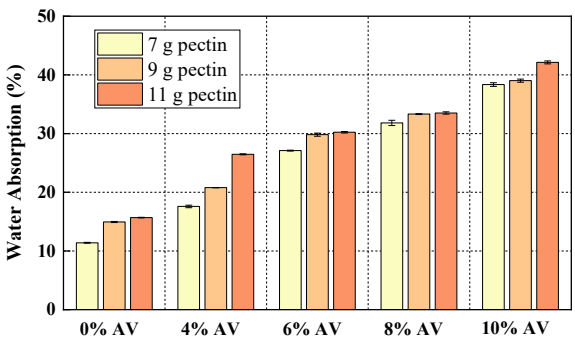


**Figure 2**: Water absorption of pectin–AV transdermal patches formulated with different pectin and AV contents. Data are expressed as mean ± SD (n = 3).

The increase in the water absorption capacity can be attributed to the hydrophilic properties of both pectin and AV. This hydrophilic nature stems from the presence of hydroxyl and carboxyl groups in both materials. These chemical groups have a strong affinity for water molecules, allowing them to be easily trapped within the microscopic pores formed by the pectin and AV matrix [33], [34]. The observed phenomenon aligns with the findings from Boanares *et al*. [35], on the preparation of pectin and cellulose cell wall to increase leaf water absorption, concluded that higher pectin content can promote faster water absorption within a film. Similarly, the addition of AV to the patch exhibited comparable effects. A study by Trang *et al*., [36] on chitosan–AV gel film demonstrated that increasing the amount AV gel in the composition resulted in both faster and greater overall water absorption.

#### *3.1.2 Swelling ratio*

The swelling capacity of the pectin–AV transdermal patch was evaluated to determine the patch's ability to retain moisture and its effectiveness in delivering active compounds. The result of the swelling experiments can be seen in Figure 3. The result showed that the addition of AV into the pectin matrix enhances the swelling capacity of the patch. The highest swelling capacity was observed in patches containing 11 g of pectin and 10% AV, reaching the swelling capacity of 91.100 ± 1.538. This represents a statistically significant increase ($p$–value = 0.021, n = 3) of 14.31% compared to the pristine pectin patch, which exhibited a swelling capacity of 79.700 ± 0.443%. This increase is biologically relevant because greater swelling enhances hydration and porosity of the matrix, which directly facilitates sustained drug diffusion through the patch.

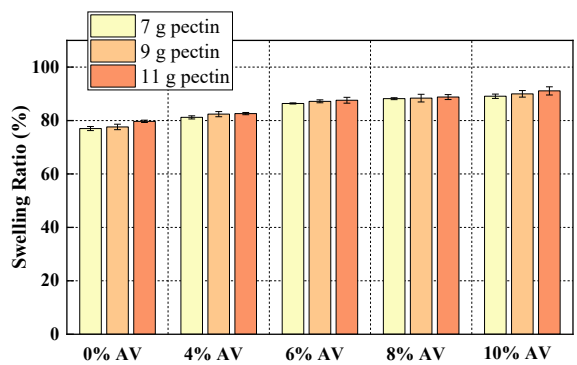


**Figure 3**: Swelling ratio of pectin–AV transdermal patches under simulated body fluid (SBF, pH 7.4, 36.5 ± 1.5 °C). Data are expressed as mean ± SD (n = 3).

The substantial increase in swelling behavior stems from the hydrophilic nature of both pectin and AV, as both substances contain hydroxyl and carboxyl groups, which have a strong affinity for water molecules. These functional groups allow the patch to absorb increased amounts of water, leading to its expansion and the swelling of its matrix [33], [34]. Additionally, the incorporation of AV creates a porous network within the polymer structure, which further facilitates water retention and results in a more pronounced swelling ratio [37]. These results are consistent with findings from the study conducted by

Sultan *et al*. [38], which examined pectin's impact on Carrageenan-based edible films and discovered higher concentration of pectin leads to an increase in swelling capability due to its water absorption properties. In a separate study, Hadi *et al*., [39] explored alginate/AV films and determined that polysaccharides, which are primary components of AV, significantly enhance the film's swelling ratio and gelling properties.

### *3.1.3 Biodegradation*

Biodegradation is a critical factor in determining the environmental impact of transdermal patches. The biodegradation of pectin–AV transdermal patch exhibited an increasing trend with more pectin and AV incorporation. The biodegradation of the 11 g pectin and 10% AV showed the highest rate of 73.330 ± 0.135 over the evaluation period. This value represents a statistically significant increase of 52.60% ($p$–value = 0.0042, n = 3) compared to the pristine pectin patch, which exhibited a biodegradation rate of 20.730 ± 0.116%. The incorporation of AV enhanced the patch's biodegradation, likely due to the synergistic effect of AV's natural decomposition properties combined with pectin's inherent biodegradability.

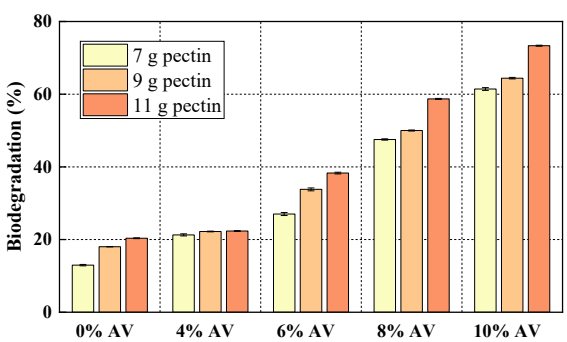


**Figure 4**: Biodegradation of pectin–AV transdermal patches over a three–month soil burial test under natural environmental conditions. Data are expressed as mean ± SD (n = 3).

The exceptional biodegradation observed can be primarily attributed to the presence of polysaccharides in both AV and pectin (Figure 4). These naturally occurring polymers are inherently biodegradable and serve as excellent substrates for microbial activity, thus accelerating the decomposition of the polymer matrix [40]. The introduction of AV into the structure likely resulted in molecular-level modifications, creating additional points of vulnerability to enzymatic action. This increased susceptibility to enzymatic breakdown consequently leads to more rapid and efficient degradation of the material.

Research by Baghersad *et al*., [41] on gelatin/AV/poly(ε–caprolactone) nanofiber scaffolds corroborates these findings. Their study reveals that the hydrophilic nature of AV facilitates water penetration, thereby accelerating biodegradation. In a separate investigation, Dayan *et al*., [42] examined AV gel incorporated into polyester resin. They found that AV-based composites exhibited the highest rate of biodegradation. This was attributed to the fibers on the specimen's surface absorbing moisture from the soil. This absorption led to fiber swelling, which ultimately resulted in the separation of the fiber from the matrix (debonding).

## 3.2 *SEM analysis of pectin-AV transdermal patch*

Morphological characterization of pectin and pectin–AV transdermal delivery matrices was executed through high–resolution scanning electron microscopy (SEM). The pristine unmodified pectin and pectin patches containing 8% AV were subjected to examine the surface topographical features via SEM evaluation. Representative SEM micrographs capturing the top surface of the biopolymer system were acquired at enhanced magnification scales of 1,000x, 3,000x, and 5,000x, as depicted in the accompanying Figure 5.

Figure 5(a)–(c) reveals the surface morphological characteristics of the pristine pectin transdermal patches with a uniformly distributed and homogeneous macromolecular network. Upon AV incorporation (Figure 5(d)–(f)), discrete particulate inclusions emerged, accompanied by substantive morphological transformations. The AV–loaded matrix exhibited enhanced surface heterogeneity, characterized by structural discontinuities, including surface roughness, cracking, and localized particulate agglomerations.

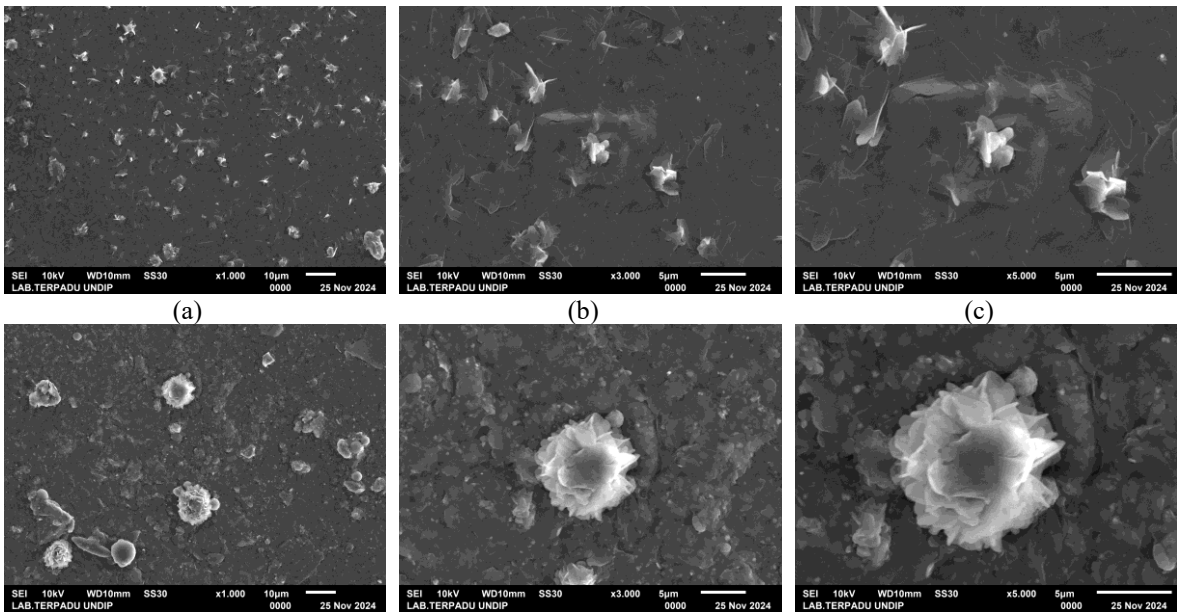


**Figure 5**: SEM morphological characterization of transdermal patches at 1,000x, 3,000x, and 5,000x magnifications: (a)–(c) pristine pectin patch; (d)–(f) pectin–AV patch (8% AV).

The morphological characteristics of patches were depended upon the agglomeration and hydrolysis patterns of polysaccharides within the AV gel [29]. Surface cracking emerged from viscosity reduction in the matrices that inhibits release of water molecules [43]. Additionally, the surface morphology exhibited unevenness, attributable to multiple lateral layering. These observations indicate a structurally divergent configuration from pristine pectin films. This manifestation was characterized by irregular, disordered, and foldable layer formations, suggesting intrinsic AV matrix integration [31]. Doping with AV leads to a notable reduction in irregular agglomeration, resulting in a combination of globular and spherical particulate configurations, accompanied by small pores and localized agglomerations [44]. Particle size approximated 8 µm, emerging from AV microglobule agglomeration with embedded pectin particles. This observation aligns with recent investigations by Begum *et al*. [45], which documented AV–Ru particle agglomerations with sizes extending up to 8,000 nm within polymeric matrices.

In terms of surface morphology, AV incorporation modified the smoothness of the pristine pectin patches, resulting in morphological alterations in the biopolymeric substrate, particularly as AV concentration increased (Figure 5(a) vs. Figure 5(d)). The rough surface topology correlates with AV gel's dispersive integration into the matrix. Incorporating AV into the pectin patch produced a heterogeneous surface via molecular interactions among the multiactive sites of both constituent compounds [31].

### 3.3 *FTIR Analysis of pectin–AV transdermal patch*

FTIR analysis was performed to examine molecular interactions and changes in functional groups resulting from the incorporation of AV and limonene drug into the pectin polymer matrix. Spectral data were collected in the range of 4000 $cm^{-1}$ to 400 $cm^{-1}$. FTIR spectroscopy was applied to both the pristine pectin patch and AV–incorporated patch. The resulting FTIR spectra of both patches are shown in Figure 6.

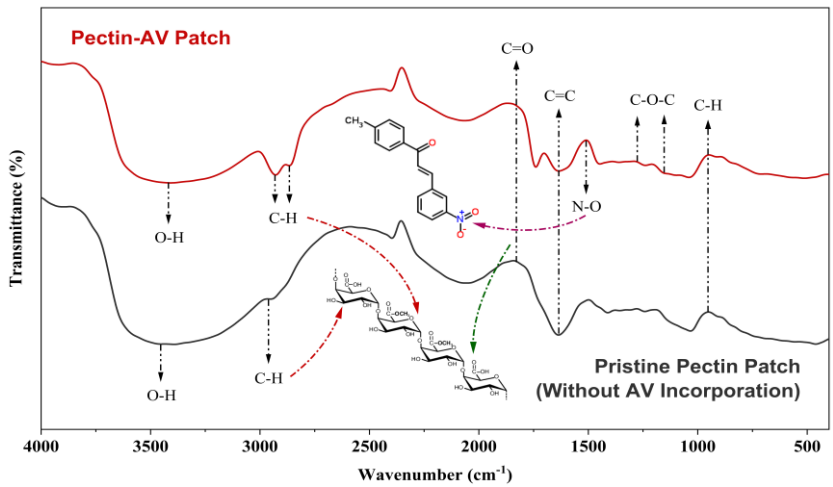


**Figure 6**: FTIR analysis of (a) pristine pectin patch (b) pectin–AV patch. Characteristic absorption bands of –OH, C–H, and C=C confirm successful incorporation of AV and limonene into the pectin matrix.

The FTIR spectrum of the pristine pectin patch revealed a broad band at 3451.76 $cm^{-1}$, characteristic of O–H stretching vibrations, indicating the presence of hydroxyl groups and adsorbed water molecules within the pectin matrix [46]. Additionally, peaks observed at 2952.18 $cm^{-1}$ correspond to the stretching vibrations of aliphatic C–H bonds, suggesting the presence of hydrocarbon chains in the pectin film components [47]. Upon incorporating AV, the transdermal patch exhibited a broad band between 3000 and 3500 $cm^{-1}$, with a peak at 3407.4 $cm^{-1}$, indicating additional hydroxyl groups (-OH) from AV constituents or phenolic groups in anthraquinones such as aloin and emodin present in AV [48]. The addition of AV resulted in new peaks at 1268.48 $cm^{-1}$, 1150 $cm^{-1}$, and 1510.33 $cm^{-1}$, indicating the presence of C-O-C glycosidic groups of deacetylated polysaccharides and chromophore functional groups [49]. The presence of these functional groups confirms the successful incorporation of active compounds from AV into the transdermal patch.

Analysis of both FTIR spectra revealed distinctive absorption bands at 2929.03 $cm^{-1}$ and 2866.34 $cm^{-1}$, which are characteristic of C–H stretching vibrations. Additionally, the spectra exhibited bands in the 1634.74 $cm^{-1}$ region, indicative of C=C stretching vibrations. These spectral features are consistent with those reported by Alipanah *et. al.,* [50] in their study on limonene–containing chitosan nanoparticles. The presence of these specific functional groups provides strong evidence for the successful incorporation of limonene into the pectin-AV transdermal patch matrix. This spectroscopic confirmation validates the effective functionalization of the patches with limonene, demonstrating the successful integration of this component into the composite structure. The spectroscopic evidence also corroborates the morphological transformations observed in SEM analysis, where the formation of heterogeneous surfaces and particulate inclusions reflects the molecular interactions between pectin, AV polysaccharides, and limonene functional groups.

### 3.4 *Mechanical properties of pectin–AV transdermal patch*

#### *3.4.1 Tensile strength*

The tensile behavior of pristine pectin and pectin–AV biopolymer transdermal patches was quantitatively assessed. The results are graphically represented in Figure 7(a). The incorporation of AV into the pectin matrix significantly modulated the tensile strength of the composite. The tensile strength exhibited a non-monotonic dependence on AV concentration with a maximum observed at 8% AV content and 11 g pectin loading. At this optimal composition, the tensile strength increased ($p$-value = 0.019, n = 3) from 0.821 ± 0.021 MPa for the pristine pectin (control) to 6.070 ± 0.008 MPa for the pectin–AV composite, representing a 7.39–fold enhancement. The observed enhancement represents a biologically significant improvement, given that superior mechanical properties are fundamental to maintaining patch structural integrity throughout handling procedures and mitigating the risk of breakage upon application, thereby facilitating

optimal patient adherence to therapeutic regimens. However, a further increase in AV concentration to 10%, while maintaining constant pectin content, resulted in a decrease of tensile strength to 4.511 ± 0.085 MPa.

Benchmarking against commercial systems provides useful context for evaluating the practical significance of the observed mechanical improvement. Polyurethane-based transdermal patches marketed under Nagase® exhibit tensile strengths in the range of 5–15 MPa with elongation at break of 100–300% [51]. Commercial hydrocolloid dressings (e.g., DuoDERM®, Tegaderm™, COMPEED®) typically exhibit modest tensile strengths (substantially 4–20 MPa in some comparative tests [52], thus the tensile performance of the optimized pectin–AV patch is comparable to established commercial patch materials, suggesting adequate robustness for practical handling and application.

The initial enhancement in tensile strength can be attributed to the dense and extensive intermolecular and intramolecular interactions within the pectin–AV composite, coupled with its inherent rigidity and stiffness. The primary mechanism responsible for this phenomenon is the efficient stress transfer between pectin and AV molecular chains [53]. The observed improvement is further facilitated by the excellent compatibility of limonene with the pectin-AV system and the homogeneous distribution of AV within the pectin matrix [54].

However, increasing the AV content to 10% results in a decline in tensile properties, likely due to oversaturation and agglomeration within the films. Bacha *et al*., [55] reported that excessive filler addition leading to decreased tensile properties is most probably a consequence of AV aggregation induced by strong hydrogen-bonding interactions between pectin molecules. Corroborating this, Rooyen *et al*., [56] reported that increasing polymer concentration did not significantly enhance tensile strength in pectin films by attributing this to a less organized polymer network. This phenomenon can also be attributed to disparities in polymer molecular mass distribution and the character of inter– and intramolecular interactions among polymeric chain structures. The elevation in AV concentration beyond an optimal threshold induces an increase in AV–AV intermolecular interactions, which compete with the existing pectin–AV interfacial bonds. This excess AV content promotes inhomogeneous dispersion within the composite matrix. Consequently, a decrement in tensile strength due to incompatibility is observed at higher AV loading levels [57].

The tensile strength behavior of the 9 g pectin formulation presents a noteworthy deviation from the general trend observed at higher pectin concentrations. While the 11 g pectin formulation exhibits the expected decline in tensile strength when AV content increases from 8% to 10% (from 6.070 ± 0.008 MPa to 4.511 ± 0.085 MPa), the 9 g pectin formulation maintains relatively stable tensile properties across this AV concentration range.

This anomalous behaviour can be attributed to the competing effects of polymer–filler interactions at different matrix densities. At the intermediate pectin concentration (9 g), the polymer matrix possesses sufficient chain mobility to accommodate the additional AV content without reaching the critical aggregation threshold observed in the more densely packed 11 g system [58]. Furthermore, the 9 g pectin matrix may represent an optimal balance between polymer chain entanglement density and filler dispersion capacity [59]. At this concentration, the pectin network maintains sufficient flexibility to redistribute stress around AV particles, while the AV loading remains below the percolation threshold that would create weak interfacial regions [60]. This suggests that the critical AV concentration for property degradation is matrix–density dependent, with more concentrated polymer systems (11 g pectin) reaching saturation limits at lower AV loadings than less concentrated systems.

The stability of tensile properties in the 9 g pectin system from 8% to 10% AV also indicates that the crosslinking efficiency between pectin and AV components remains optimal within this composition by avoiding the competitive hydrogen bonding interactions that destabilize the 11 g system at higher AV concentrations [61].

### *3.4.2 Elongation at break*

Figure 7(b) illustrates the inverse relationship between pectin–AV incorporation and elongation at break. The maximum elongation at break, observed in the pristine 11 g pectin patch, was quantified as 129.763 ± 0.568%. This value exhibited a statistically significant decrease of 86.88% ($p$-value = 0.032, n = 3) to a minimum of 17.024 ± 0.177% for the 11 g pectin patch containing 8% AV. This negative correlation between elongation at break and AV concentration is consistent with established trends in composite materials, where

the incorporation of reinforcing particulates typically results in a reduction of polymer chain mobility and consequently diminished elongation capacity [56].

The observed decrease in elongation at break with elevated filler concentration can be predominantly ascribed to the reinforcement effect of highly crystalline and rigid AV particles on the comparatively flexible chains of the pectin matrix. This mechanism significantly restricts the overall chain mobility within the biocomposite systems [62]. Moreover, the robust matrix–filler adhesion may contribute to diminished ductility and extensibility. This clarifies the noted reduced deformability resulting from substantial interfacial adhesion between matrix and fillers [63]. The AV particulates, possessing inferior deformability relative to the pectin matrix, in conjunction with potent interactions between particulate and matrix molecules, constrain the ability of pectin chains to extend under tensile loading.

The elongation at break exhibited its maximum value in the absence of AV (0% AV concentration). Huang *et al*., [64] attribute these decreases in elongation at break to deacetylation and crosslinking phenomena. It was found that the formation of compact bonds results in a more rigid structure, as the crosslinked pectin enhances strength but reduces the film toughness. Singh *et al*., [65] hypothesize that AV establishes interactions with polysaccharide hydroxyl moieties, thus facilitating enhanced interfacial compatibility between polymeric constituents and augmenting the tensile properties of polysaccharide–based matrices. Furthermore, it has been demonstrated that AV provides a mucilaginous polymeric network that acts as a crosslinking agent within the films. This finding aligns with previous studies [66], [67], corroborating the role of AV in modifying the mechanical properties of pectin–based composites. The combined effects of these mechanisms–namely, the formation of a more rigid structure through compact bonding, enhanced crosslinking, and the introduction of a mucilaginous network–collectively contribute to the observed inverse relationship between AV concentration and elongation at break in the pectin–AV system.

### *3.4.3 Young's modulus*

The elasticity of pristine pectin and pectin–AV was evaluated to examine the impact of AV incorporation on patch flexibility and resilience. Figure 7(c) graphically represents these findings, revealing significant modulation of AV incorporation into the matrix. At 0% AV, the Young's modulus increased with pectin concentration, from 0.327 ± 0.008 MPa to 0.734 ± 0.015 MPa. This trend persisted across all AV concentrations, indicating that higher pectin content consistently resulted in stiffer patches. The addition of AV generally increased the Young's modulus. At 8% of AV incorporation, the maximum Young's modulus with a maximum of 30.780 ± 0.642 MPa at 11 g of pectin, representing a substantial increase ($p$-value = 0.0038, n = 3) in stiffness compared to the AV–free patches. Notably, the relationship between AV concentration and Young's modulus was non–linear. The modulus peaked at 8% AV for all pectin concentrations, followed by a decrease at 10% AV. This trend was particularly pronounced for the 11 g pectin formulation, where the Young's modulus increased from 0.734 ± 0.015 MPa (0% AV) to 30.780 ± 0.642 MPa (8% AV), before decreasing to 22.351 ± 0.017 MPa at 10% AV.

The increase in stiffness with higher pectin concentrations can be attributed to the molecular structure and behavior of pectin in solution. Pectin, as a complex polysaccharide forms a network of interconnected chains through hydrogen bonding and electrostatic interactions [68]. Elevating the pectin concentration diminishes the intermolecular distances and amplifies intermolecular forces, resulting in an augmented quantity of intermolecular junctions [69]. This large number of networks offers greater resistance to deformation under stress, manifesting as increased stiffness. The observed linear relationship between pectin concentration and stiffness suggests that this network formation occurs consistently across the range of concentrations studied.

Integration of AV within the pectin matrix typically yielded an elevation in Young's modulus, indicating enhanced rigidity of the patches. The observed correlation between tensile strength (Figure 7(a)) and Young's modulus (Figure 7(c)) in the pectin–AV biopolymer system reflects fundamental structure–property relationships in polymer mechanics. Both parameters are intrinsically linked to intermolecular interactions and crosslink density within the matrix. The parallel improvement indicates that AV incorporation strengthens the structural integrity without compromising flexibility. Young's modulus is recognized to increase proportionally with polymerization or crosslinking density of a material. Elements contributing to heightened crosslinking

density include monomer and crosslinker concentrations. As concentration escalates, material density increases, culminating in superior mechanical integrity, specifically in this instance, the Young's modulus [37]. The remarkable increase in Young's modulus ($p$-value = 0.0088, n = 3) from 0.734 ± 0.015 MPa to 30.780 ± 0.642 MPa at 11 g pectin illustrates the significant reinforcement capacity of AV within this composite system. The correlation between AV concentration and Young's modulus exhibited a non–linear pattern, with a peak observed at 8% AV, followed by a decrease at 10% AV. This unexpected behavior might be attributed to the plasticizing properties of AV when present in higher quantities. Polysaccharides as a principal component of AV can induce an expansion of intermolecular spaces, thereby enhancing molecular mobility, resulting in a reduction of crystallinity degree. Consequently, this molecular reorganization may result in a decrease in the Young's modulus [70].

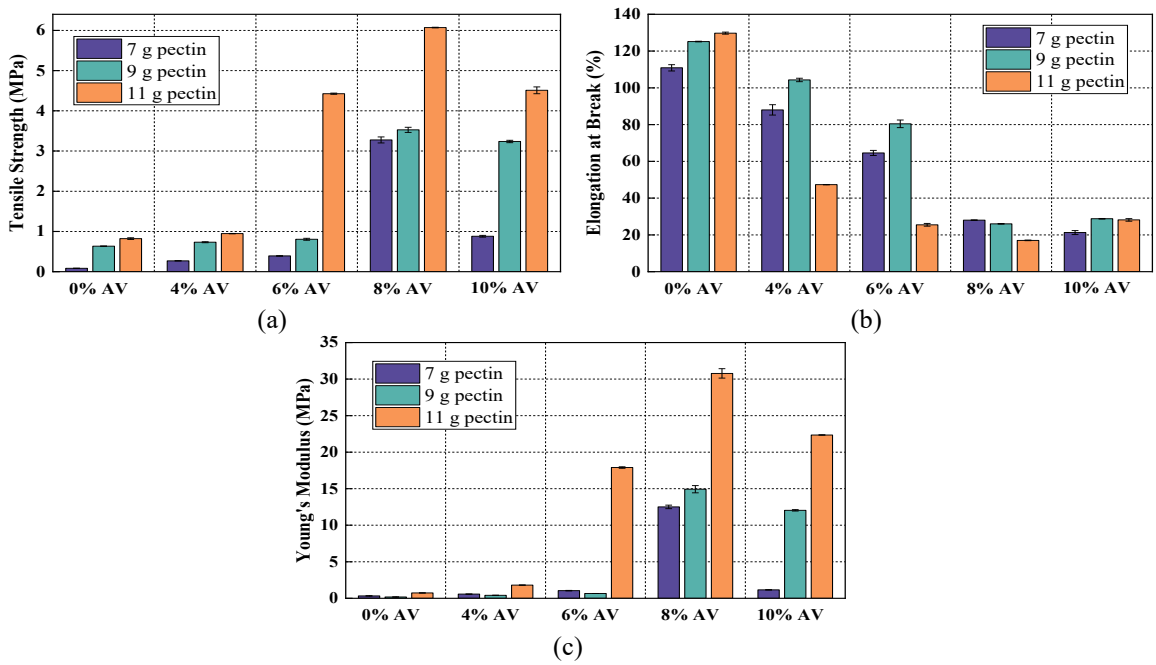


**Figure 7**: Mechanical properties of pectin–AV transdermal patches as a function of filler incorporation: (a) Tensile strength, (b) Elongation at break, and (c) Young's modulus. Data are expressed as mean ± SD (n = 3).

### 3.5 *In vitro drug release kinetics*

The drug release studies were conducted in Franz diffusion cells with a 20 mL capacity and the release kinetics were determined. The release studies were performed over a 120–h period to achieve a constant release percentage. The investigation focused on 8% AV pectin–based transdermal patches to evaluate their release profiles. Figure 8 illustrates the *in vitro* release profiles of limonene across a synthetic membrane.

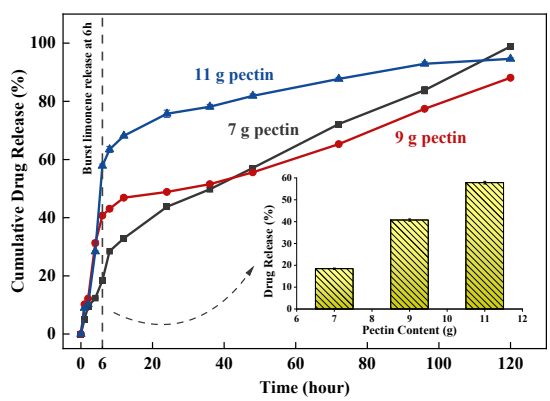


**Figure 8**: *in vitro* release profiles of limonene from 8% AV pectin–based transdermal patches, measured over 120 h using a Franz diffusion cell.

The composition of drug formulations exerts a significant influence on release kinetics and profiles [71]. The lowest pectin content of 7 g demonstrated efficacy in controlling initial burst release, with approximately 18.435 ± 0.307% of limonene released within 6 hours. However, such minimal drug loading compromises product efficiency and economic viability. This system exhibited a maximum release capacity of 98.873 ± 0.596% over a 120–h period. A 9 g loading resulted in moderated release (40.734 ± 0.519% after 6 h) but demonstrated the lowest cumulative release at 120 h. As such, an 11 g pectin loading was determined to be optimal, displaying enhanced initial burst release kinetics (57.849 ± 0.60% within 6 h). This formulation exhibited significantly moderate limonene release compared to other compositions ($p$-value = 0.0042, n = 3). The 11 g loading, achieving 94.61 ± 0.297% cumulative release over 120 h, emerged as the optimal formulation, balancing initial burst release and controlled drug delivery. Consequently, this pectin concentration was selected for the subsequent release kinetics analyses.

The pectin–AV biopolymer system was found to enhance drug release efficacy. The inclusion of AV functions as a chemical permeation enhancer, facilitating augmented drug transport by reducing the skin barrier, thus enabling efficacious and safe transdermal therapeutic delivery [72]. This indicates the use of AV in combination with pectin films for efficient limonene liberation. The release kinetics of limonene underwent subsequent analysis using three mathematical models (zero–order, first-order, Korsmeyer–Peppas). The obtained release data were plotted and evaluated to determine the most appropriate kinetic model for elucidating the drug diffusion process.

The release rate parameters and constants obtained from various kinetic models are presented in Figure 9. Analysis of regression coefficient values indicated that the Korsmeyer–Peppas model most accurately described the drug release kinetics. The observed n value of 0.472 suggests an anomalous or non–Fickian diffusion process for limonene release from the biopolymer matrix. This non–Fickian diffusion mechanism likely results from inadequate mobility of polymer chains that impedes rapid water penetration into the polymer core [73]. The proposed release mechanism for limonene involves dethreading from the pectin chain through swelling, coupled with enhanced penetration facilitated by AV presence, resulting in limonene erosion and subsequent drug diffusion [74]. Similar release capacities have been observed in other systems reported in literature, such as pectin-based silver nanocomposite films [75]. These systems exhibited a drug release capacity of 94.33 ± 2.12% in phosphate buffer saline solution (PBS) over a 5-day period, also following non-Fickian diffusion kinetics. Nanoemulsions of finger citron essential oil (FCEO) exhibited a d-limonene release percentage of 95% within 5 h [76] with maximal release occurring at pH 1.2 and following the Ritger–Peppas model. Amylose nanocarriers loaded with limonene extracted from encapsulated orange peel oil effectively released 79% of limonene to simulated intestinal fluid (SIF) over 6 h [77]. These nanostructures were prepared using a modified sonication–thermal method. Considering these literature reports, the present pectin–AV system demonstrates an enhanced release profile with an approximately 95% release in a controlled manner over 120 h (5 days). This enhanced release profile represents a significant advantage for the application of the present system in the controlled delivery of hydrophilic drugs.

However, several methodological limitations must be acknowledged in the present release study design. While benzoylated dialysis membrane provides a reproducible assessment of formulation–controlled release, it does not reproduce the skin barrier; hence, these data reflect in vitro release rather than in vivo transdermal permeation. Conservative calculations based on typical patch loadings (1–10 mg per 1 $cm^2$) and empirical limonene solubility in PBS (≈0.013 mg $mL^{-1}$) indicate that receptor used herein would preserve sink conditions when the receptor medium's solubility were substantially enhanced (for example through surfactant/cosolvent addition) or the receptor volume increased to the $10^2$ to $10^3$ mL range [78], [79]. Consequently, future confirmatory experiments will 1) measure limonene saturation solubility in the chosen receptor medium at 37 °C, 2) use an appropriately sized receptor volume or a surfactant–supplemented medium with the solubility reported, and 3) perform permeation studies using excised skin or *in vivo* models to evaluate pharmacokinetics, therapeutic efficacy, relevant transdermal flux, and skin safety to confirm the clinical applicability of the developed system.

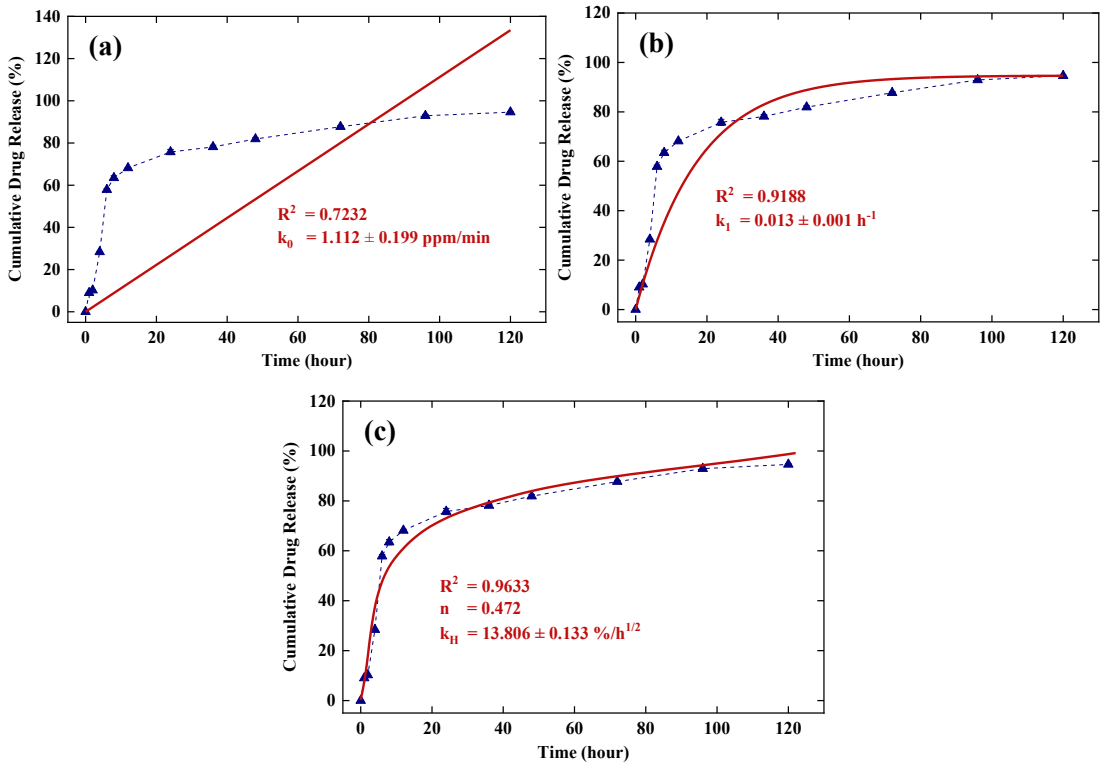


**Figure 9**: Release kinetics of limonene from pectin–AV transdermal patches fitted to mathematical models: (a) Zero–order, (b) First-order, and (c) Korsmeyer–Peppas. The best fit was obtained with the Korsmeyer–Peppas model (n = 0.472), indicating a non-Fickian diffusion mechanism.

### 3.6 *Cost estimation*

The economic viability of scaled–up pectin–AV transdermal patch fabrication has been assessed via cost evaluation. The manufacturing apparatus, consisting of a 10×100 L stainless–steel liquid mixing vessel equipped with mechanical agitation and electric thermal regulation, functions on a 330–day yearly production schedule. Table 1 presents the projected capital investment and operational expenditures.

Cost estimates were based on market prices obtained from Indonesian suppliers in June 2025. Food–grade pectin pricing was sourced from PT Phy Edumedia (Malang, Indonesia) at approximately 45–50 USD/kg for low methoxyl pectin. Fresh AV leaves were priced at local markets in Medan, Indonesia, at 2–3 USD/kg. Glycerol and other chemical costs were based on Merck KGaA distributor pricing in Indonesia. The 330–day operational schedule assumes standard industrial practice with allowances for maintenance downtime (30 days) and seasonal variations (5 days). Equipment costs were obtained from Indonesian manufacturing equipment suppliers. However, the economic model was limited by assuming steady-state production without considering startup costs, learning curve effects, or market penetration challenges.

Capital expenditure distribution assessment indicates that the pectin–AV manufacturing apparatus (mixing vessel) represents the predominant investment at 65.44%, succeeded by the roll press–feeder for patch production (23.38%) and the tray desiccator (6.54%). The allocation of capital investments emphasizes the significance of equipment specification and capacity in determining overall capital investment, with the production vessel constituting the primary cost component due to its essential function in patch manufacture. The operational expenditures are predominantly influenced by electrical consumption, comprising 67.78% of total operational disbursements. The predominance of energy costs within the operational budget emphasizes the imperative for energy conservation strategies and potentially investigating renewable energy alternatives to enhance long–term

operational sustainability. Raw material costs, encompassing food–grade pectin, raw AV, glycerol, and lime as limonene carrier, represent 16.07% of the operational expenditures. Analysis on per–liter basis generates the following parameters: estimated capital investment of 1.9 USD/L, operational cost of 0.6 USD/L, gross profit of 2.5 USD/L, and net profit of 2.8 USD/L. The positive revenue margin indicates that the scaled–up manufacture of pectin–AV transdermal patches exhibits promising commercial viability even at the presented scale of operations.

**Table 1**: Cost analysis of scaled–up pectin–AV patches fabrication process (10×100 L capacity).

| **Direct Capital Cost (USD)** | **Rate** |
|---|---|
| Mixing vat, 10×100 L capacity | 8,350.0 |
| Dehydrator, 2×20-tray dryer | 834.1 |
| Roll feeder | 2,982.9 |
| Framework | 30.4 |
| Automation and control system | 182.4 |
| Piping, hosing, and connection components | 152.0 |
| Workforce expenditures | 228.0 |
| **Total** | **12,759.7** |
| | |
| **Operating Cost (USD/year)** | |
| Electrical | 2,608.8 |
| Maintenance | 621.7 |
| Chemicals | 618,4 |
| **Total** | **3,848.9** |
| | |
| **Profit Gained (USD/year)** | |
| Raw pectin-AV gel sales | 10,488.1 |
| Pectin-AV-limonene transdermal patches sales | 24,472.3 |
| Lime peel waste, for fertilizer (to be outsourcing) | 1.3 |
| AV leaf waste, for fertilizer (to be outsourcing) | 0.9 |
| **Total** | **34,962.7** |
| | |
| **Cost per Liter (USD/L)** | |
| Capital Cost | 1.9 |
| Operating Cost | 0.6 |
| **Total Cost** | **2.5** |
| Profit Gained | 5.3 |
| **Net Profit** | **2.8** |

## 4 Conclusions

This study successfully demonstrates the development of a novel pectin–based transdermal drug delivery system enhanced by *Aloe vera* (AV) incorporation, thus addressing the inherent limitations of conventional pectin matrices. The incorporation of AV extract significantly improved the mechanical properties, evidenced by a 7.39–fold increase in tensile strength and optimized Young's modulus of 30.780 ± 0.642 MPa, ensuring enhanced structural integrity and durability. Furthermore, the optimized formulation of 11 g pectin and 10% AV exhibited superior physicochemical characteristics, including controlled swelling, moisture content, and biodegradation profiles, alongside a robust in vitro performance, achieving a cumulative limonene release of 94.61 ± 0.297% over 120 h via non–Fickian diffusion mechanisms. FTIR spectroscopy confirmed successful molecular integration of the AV, pectin, and limonene components, while SEM analysis highlighted the globular and spherical particulate configurations with a particle size of approximately 8 μm, as well as heterogeneity of the matrix. The economic assessment substantiated the industrial feasibility of the approach with an advantageous cost–to–profit proportion yielding net earnings of 2.8 USD/L. However, several limitations must be acknowledged for future developments. The formulation exhibited a high initial burst release, which may affect controlled drug delivery and skin irritation potential remains untested. Superior release profile requires validation against commercial transdermal patches under standardized conditions. Additionally, comprehensive *in vivo* investigations to evaluate efficacy, safety, and long–term stability remain critical to advancing clinical and

commercial applications. Future studies will therefore focus on *in vivo* evaluation in appropriate animal models to investigate pharmacokinetics, therapeutic efficacy, skin irritation, and systemic safety. These efforts will be crucial in translating the developed formulation toward clinical and commercial application. Collectively, these findings establish a promising platform for the development of biodegradable and cost–effective transdermal drug delivery systems tailored for pharmaceutical and cosmetic applications.

**Acknowledgments**

The research was funded by the Institute for Research at Universitas Sumatera Utara (LP-USU) through Government Collaborative Research 'Penelitian Kolaborasi Pemerintah' TALENTA USU scheme, as per research grant number 73/UN.5.4.10.S/PPM/KP–TALENTA/RB1/2024. The authors sincerely acknowledge and express gratitude for the research sponsorship enabling the presented work.

**Author Contributions**

N.F.D.: Conceptualization, Data curation, Resources, Writing–original draft; M.M.: Formal analysis, Investigation, Visualization, Writing–review & editing; T.M.T.: Investigation, Project administration, Visualization; I.M.P.: Formal analysis, Resources, Writing–original draft; J.H.: Formal analysis, Writing–review & editing; P.M.: Validation; M.T.A.F: Supervision, Validation; R.V.: Investigation, Methodology, Project administration; S.K.W.: Supervision, Validation. All authors have read and agreed to the published version of the manuscript.

**Conflicts of Interest**

The authors declare no conflict of interest.

**References**

[1] H. Qin et al., "Advances of transdermal drug delivery system based on extracellular vesicles," *Journal of Drug Delivery Science and Technology*, vol. 105, 2025, doi: 10.1016/j.jddst.2025.106647.

[2] M. S. Huang, P. Chanapongpisa, P. Yasurin, K. Kitsubthawee, J. Phetsom, and Ir. Lindayani, "Centella asiatica extract loaded BSA nanoparticles using the organic and conventional C. asiatica to improve bioavailability activity and drug delivery system," *Applied Science and Engineering Progress*, vol. 13, no. 1, pp. 11–18, 2020, doi: 10.14416/j.asep.2020.01.001.

[3] R. Chakraborty, N. Afrose, and K. Kuotsu, "Novel synergistic approaches of protein delivery through physical enhancement for transdermal microneedle drug delivery: A review," *Journal of Drug Delivery Science and Technology*, vol. 84, 2023, doi: 10.1016/j.jddst.2023.104467.

[4] W. Y. Jeong, M. Kwon, H. E. Choi, and K. S. Kim, "Recent advances in transdermal drug delivery systems: A review," *Biomaterials Research*, vol. 25, p. 24, 2021, doi: 10.1186/s40824-021-00226-6.

[5] T. Karve, A. Dandekar, V. Agrahari, M. M. Peet, A. K. Banga, and G. F. Doncel, "Long-acting transdermal drug delivery formulations: Current developments and innovative pharmaceutical approaches," *Advanced Drug Delivery Reviews*, vol. 210, 2024, doi: 10.1016/j.addr.2024.115326.

[6] M. S. Amiri, V. Mohammadzadeh, M. E. T. Yazdi, M. Barani, A. Rahdar, and G. Z. Kyzas, "Plant-based gums and mucilages applications in pharmacology and nanomedicine: A review," *Molecules*, vol. 26, pp. 1770, doi: 10.3390/molecules26061770.

[7] Z. Karim, P. Karwa, and S. R. R. Hiremath, "Polymeric microneedles for transdermal drug delivery- a review of recent studies," *Journal of Drug Delivery Science and Technology*, vol. 77, 2022, doi: 10.1016/j.jddst.2022.103760.

[8] T. Suwandecha and P. Changklang, "Formulation development and characterization of a transdermal patch containing Crinum asiaticum leaves extract," *Journal of Applied Pharmaceutical Science*, vol. 13, pp. 207–213, 2023, doi: 10.7324/JAPS.2023.151643.

[9] N. F. Dalimunthe, S. K. Wirawan, M. Michael, T. M. Tjandra, M. T. Al Fath, and R. Sidabutar, "Pectin-carbonate hydroxyapatite composite films as a potential drug delivery system for cinnamaldehyde: Characterization and release kinetics modeling," *Case Studies in Chemical and Environmental Engineering*, vol. 10, p. 100905, 2024, doi: 10.1016/j.cscee.2024.100905.

[10] W. M. Kedir, E. M. Deresa, and T. F. Diriba, "Pharmaceutical and drug delivery applications of pectin and its modified nanocomposites,"

*Heliyon*, vol. 8, 2022, doi: 10.1016/j.heliyon.2022.e10654.

[11] Z. Jader, F. T. Yazdi, S. A. Mortazavi, and A. Kocheki, "Effects of glycerol and sorbitol on a novel biodegradable edible film based on Molva sylvestris flower gum," *Food Science and Nutrition*, vol. 11, pp. 991–1000, 2023, doi: 10.1002/fsn3.3134.

[12] I. Backsay et al., "Formulation and evaluation of transdermal patches containing BGP-15," *Pharmaceutics*, vol. 16, p. 36, 2024, doi: 10.3390/pharmaceutics16010036.

[13] W. A. Asfaw, K. D. Tafa, and N. Satheesh, "Optimization of citron peel pectin and glycerol concentration in the production of edible film using response surface methodology," *Heliyon*, vol. 9, 2023, doi: 10.1016/j.heliyon.2023.e13724.

[14] T. Nisar et al., "Citrus pectin films enriched with thinned young apple polyphenols for potential use as bio-based active packaging," *CyTA – Journal of Food*, vol. 17, pp. 695–705, 2019, doi: 10.1080/19476337.2019.1640798.

[15] S. Andini, E. Rustiani, and U. Lathifah, "Formulation and In-vitro penetration test of ketoprofen patch with addition aloe vera powder (Aloe vera L.) bioenhancer," *Fitofarmaka*, vol. 14, pp. 51–58, 2024, doi: 10.33751/jf.v14i1.9874.

[16] R. A. Jiménez, D. Millán, A. Sosnik, and M. R. Fontanilla, "Aloe vera–eluting collagen I microgels: physicochemical characterization and in vitro biological performance," *Materials Today Chemistry*, vol. 23, 2022, doi: 10.1016/j.mtchem.2021.100722.

[17] M. A. Bhutkar, S. D. Bhinge, D. S. Randive, O. Nayakal, and P. Patil, "Evaluation of dimethylsulfoxide and Aloe vera as penetration enhancers for cutaneous application of lidocaine," *Ars Pharmaceutica*, vol. 60, pp. 85–92, 2019, doi: 10.30827/ars.v60i2.8084.

[18] J. Sainy, U. Atneriya, J. L. Kori, and R. Maheshwari, "Development of an aloe vera-based emulgel for the topical delivery of desoximetasone," *Turkish Journal of Pharmaceutical Sciences*, vol. 18, pp. 465–475, 2021, doi: 10.4274/tjps.galenos.2020.33239.

[19] N. A. Charoo, A. A. A. Shamsher, K. Kohli, K. Pillai, and Z. Rahman, "Improvement in bioavailability of transdermally applied flurbiprofen using tulsi (*Ocimum sanctum*) and turpentine oil," *Colloids and Surfaces B: Biointerfaces*, vol. 65, pp. 300–307, 2008, doi: 10.1016/j.colsurfb.2008.05.001.

[20] X. F. Chen et al., "The pharmacological effects and potential applications of limonene from citrus plants: A review," *Natural Product Communications*, vol. 19, 2024, doi: 10.1177/1934578X241254229.

[21] A. A. Maan, Z. F. R. Ahmed, M. K. I. Khan, A. Riaz, and A. Nazir, "Aloe vera gel, an excellent base material for edible films and coatings," *Trends in Food Science and Technology*, vol. 116, pp. 329–341, 2021, doi: 10.1016/j.tifs.2021.07.035.

[22] D. N. Iqbal et al., "Polymeric membranes of chitosan/aloe vera gel fabrication with enhanced swelling and antimicrobial properties for biomedical applications," *Dose-Response*, vol. 21, 2023, doi: 10.1177/15593258231169387.

[23] M. T. A. Fath et al., "Bio-sourced black Soldier Fly (*Hermetia illucens*) maggot chitosan/PVA/PAN-based polymer electrolyte membrane for sustainable energy storage applications," *Applied Science and Engineering Progress*, vol. 18, no. 1, 2025, Art. no. 7485, doi: 10.14416/j.asep.2024.07.002.

[24] ASTM International, "ASTM D570-98: Standard Test Method for Water Absorption of Plastics," ASTM International, West Conshohocken, PA, 1998.

[25] M. Q. Bedregal, E. M. de Jara, H. P. Cordero, and L. M. Zanardi, "Development and characterization of novel packaging films from composite mixtures of rice-starch, tara gum and pectin," *International Journal of Food Science & Technology*, vol. 60, no. 3, pp. 1153–1162, Jan. 2023, doi: 10.1007/s13197-023-05669-4.

[26] H. Jodati, Z. Evis, A. Tezcaner, A. Z. Alshemary, and A. Motamen, "3D porous bioceramic based boron-doped hydroxyapatite/baghdadite composite scaffolds for bone tissue engineering," *Journal of the Mechanical Behavior of Biomedical Materials*, vol. 140, p. 105722, 2023, doi: 10.1016/j.jmbbm.2023.105722.

[27] Z. Terzopoulou, A. Michopoulou, A. P. E. Koliakou, and D. Bikiaris, "Preparation and evaluation of collagen-based patches as curcumin carriers," *Polymers*, vol. 12, p. 2393, 2020, doi: 10.3390/polym12102393.

[28] F. Convertino et al., "The fate of post-use biodegradable PBAT-based mulch films buried in agricultural soil," *Science of The Total Environment*, vol. 948, p. 174697, 2024, doi: 10.1016/j.scitotenv.2024.174697.

[29] O. García-Depraect et al., "Biodegradation of bioplastics under aerobic and anaerobic aqueous conditions: Kinetics, carbon fate and particle size effect," *Bioresource Technology*, vol. 344, pp. 126265, 2022, doi: 10.1016/j.biortech.2021.126265.

[30] ASTM International, "ASTM D882-10: Standard Test Method for Tensile Properties of Thin Plastic Sheeting," ASTM International, West Conshohocken, PA, 2010.

[31] S. Carrasco, L. González, M. Tapia, B. F. Urbano, C. Aguayo, and K. Fernández, "Enhancing alginate hydrogels as possible wound-healing patches: The synergistic impact of reduced graphene oxide and tannins on mechanical and adhesive properties," *Polymers*, vol. 16, p. 1081, 2024, doi: 10.3390/polym 16081081.

[32] A. K. Kodoth, V. M. Ghate, S. A. Lewis, B. Prakash, and V. Badalamoole, "Pectin-based silver nanocomposite film for transdermal delivery of Donepezil," *International Journal of Biological Macromolecules*, vol. 134, pp. 269–279, 2019, doi: 10.1016/j.ijbiomac.2019.04.191.

[33] Q. Liu et al., "A high-performance watermelon skin ion-solvating membrane for electrochemical CO2 reduction," *Nature Communications*, vol. 15, p. 6722, 2024, doi: 10.1038/s41467-024-51139-6.

[34] M. Chelu et al., "High-content aloe vera based hydrogels: Physicochemical and pharmaceutical properties," *Polymers*, vol. 15, p. 1312, 2023, doi: 10.3390/polym15051312.

[35] D. Boanares, B. G. Ferreira, A. R. Kozovits, H. C. Sousa, R. M. S. Isaias, and M. G. C. França, "Pectin and cellulose cell wall composition enables different strategies to leaf water uptake in plants from tropical fog mountain," *Plant Physiology and Biochemistry*, vol. 122, pp. 57–64, 2018, doi: 10.1016/j.plaphy.2017.11.005.

[36] T. Y. D. Trang, H. T. Dzung, T. T. Huong, L. Q. Dien, D. T. Hanh, and H. T. N. Phuong, "Preparation and characterization of chitosan/ aloe vera gel film for fresh fruit preservation," *E3S Web of Conferences*, vol. 443, p. 02003, 2023, doi: 10.1051/e3sconf/202344302003.

[37] A. Mahmood et al., "Sustained drug delivery, development, characterization, and *in vitro* evaluation," *Gels*, vol. 9, p. 474, 2023, doi: 10.3390/gels9060474.

[38] R. A. Sultan, A. N. F. Rahman, A. Dirpan, and A. Syarifuddin, "Physical, mechanical, barrier, antibacterial properties, and functional group of carrageenan-based edible film as influenced by pectin from *Dillenia serrata* fruit peel and curcumin," *Current Research in Nutrition and Food Science Journal*, vol. 11, pp. 1308–1321, 2023, doi: 10.12944/CRNFSJ.11.3.32.

[39] A. Hadi, A. Nawab, F. Alam, and K. Zehra, "Alginate/aloe vera films reinforced with tragacanth gum," *Food Chemistry: Molecular Sciences*, vol. 4, 2022, doi: 10.1016/j.fochms. 2022.100105.

[40] Z. U. Arif, "The role of polysaccharide-based biodegradable soft polymers in the healthcare sector," *Advances in Industrial and Engineering Polymer Research*, 2024, doi: 10.1016/j.aiepr. 2024.05.001.

[41] S. Al-Hajri, B. M. Negash, M. M. Rahman, M. Haroun, and T. M. Al-Shami, "Perspective review of polymers as additives in water-based fracturing fluids," *ACS Omega*, vol. 7, pp. 7431–7443, 2022, doi: 10.1021/acsomega.1c06739.

[42] M. A. R. Dayan, M. M. Habib, M. M. Uddin, M. Khatun, M. S. Hossain, and M. A. Rashid, "Characterization of aloe vera gel incorporated unsaturated polyester resin jute-cotton fabric composites for enhanced biodegradability, flexibility, and insulation properties," *Heliyon*, vol. 10, 2024, doi: 10.1016/j.heliyon.2024.e35261.

[43] A. Izadi, H. Rashedi, R. Ghafarzadegan, and R. Hajiaghaee, "Evaluation the effect of enzymatic process on the edible aloe vera gel viscosity using commercial cellulase," *Journal of Applied Biotechnology Reports*, vol. 2, pp. 299–303, 2015.

[44] M. H. Rashid, S. I. Sujoy, M. S. Rahman, and M. J. Haque, "Aloe vera assisted green synthesis of Ag and Cu co-doped ZnO nanoparticles and a comprehensive analysis of their structural, morphological, optical, electrical and antibacterial properties," *Heliyon*, vol. 10, 2024, doi: 10.1016/ j.heliyon.2024.e25438.

[45] T. Begum et al., "Aloe vera gel mediated green synthesis of ruthenium nanoparticles and their potential anticancer activity," *Next Nanotechnology*, vol. 7, 2025, doi: 10.1016/j.nxnano.2024.100095.

[46] S. Mohanasundaram et al., "Extraction of pectin from Ethiopian prickly pear fruit peel and its potency for preparing of cellulose-reinforced biofilm," *Biomass Conversion and Biorefinery*, vol. 14, pp. 32133–32147, 2024, doi: 10.1007/ s13399-023-04996-y.

[47] V. F. Ursachi, M. Oroian, and M. Spinei, "Development and characterization of biodegradable films based on cellulose derivatives and citrus pecting: A comparative study," *Industrial Crops and Products*, vol. 219, 2024, doi: 10.1016/j.indcrop.2024.119052.

[48] D. Bajer, K. Janczak, and K. Bajer, "Novel starch/chitosan/aloe vera composites as promising biopackaging materials," *Journal of Polymers and the Environment*, vol. 28, pp. 1021–1039, 2020, doi: 10.1007/s10924-020-01661-7.

[49] S. Chismirina et al., "Study of formulation and FTIR analysis of aloe vera gel for periodontal disease therapy," *Journal of Community and Preventive Dentistry*, vol. 2, pp. 7–13, 2024.

[50] H. Alipanah, M. Farjam, E. Zarenezhad, G. Roozitalab, and M. Osanloo, "Chitosan nanoparticles containing limonene and limonene-rich essential oils: Potential phytotherapy agents for the treatment of melanoma and breast cancers," *BMC Complementary Medicine and Therapies*, vol. 21, p. 186, 2021, doi: 10.1186/s12906-021-03362-7.

[51] Nagase ChemteX, "Characteristics of Polyurethane (elongation, strength, shock absorption) and comparison with other materials," 2025.

[52] P. Mohite et al., "Polymeric hydrogel sponges for wound healing applications: A comprehensive review," *Regenerative Engineering and Translational Medicine*, vol. 10, pp. 416–437, 2024, doi: 10.1007/s40883-024-00334-4.

[53] Y. C. Ching, A. Rahman, K. Y. Ching, N. L. Sukiman, and C. H. Chuah, "Preparation and characterization of polyvinyl alcohol-based composite reinforced with nanocellulose and nanosilica," *BioResources*, vol. 10, pp. 3364–3377, 2015, doi: 10.15376/biores.10.2.3364-3377.

[54] K. A. Jodhani and M. Nataraj, "Synergistic effect of Aloe gel (*Aloe vera* L.) and Lemon (*Citrus Limon* L.) peel extract edible coating on shelf life and quality of banana (*Musa* spp.)," *Journal of Food Measurement and Characterization*, vol. 15, pp. 2318–2328, 2021, doi: 10.1007/s11694-021-00822-z.

[55] E. G. Bacha, H. D. Demsash, L. D. Shumi, and B. E. Debesa, "Investigation on reinforcement effects of nanocellulose on the mechanical properties, water absorption capacity, biodegradability, optical properties, and thermal stability of a polyvinyl alcohol nanocomposite film," *Advances in Polymer Technology*, vol. 2022, 2022, doi: 10.1155/2022/6947591.

[56] B. V. Rooyen, M. D. Wit, G. Osthoff, J. V. Niekerk, and A. Hugo, "Effect of pH on the mechanical properties of single-biopolymer mucilage (*Opuntia ficus-indica*), pectin and alginate films: Development and mechanical characterisation," *Polymers*, vol. 15, p. 4640, 2023, doi: 10.3390/polym15244640.

[57] R. K. Deshmukh, P. Kumar, R. Tanwar, and K. K. Gaikwad, "Pectin polyvinylpyrrolidone based antimicrobial and antioxidant nanocomposite film impregnated with titania nanoparticles and bael shell extract," *Food and Bioprocess Technology*, vol. 15, pp. 2839–2853, 2022, doi: 10.1007/s11947-022-02922-0.

[58] R. Chen et al., "Improving carrier mobility of near-amorphous donor–acceptor conjugated polymer thin films via promoting intensive and continuous polymer aggregations," *Macromolecules*, vol. 56, pp. 5356–5368, 2023, doi: 10.1021/acs.macromol.3c00316.

[59] M. Fiedot-Toboła, A. Dmochowska, R. Jędrzejewski, W. Stawiński, B. Kryszak, and J. Cybińska, "Pectin-organophilized ZnO nanoparticles as sustainable fillers for high-density polyethylene composites," *International Journal of Biological Macromolecules*, vol. 182, pp. 1832–1842, 2021, doi: 10.1016/j.ijbiomac.2021.05.133.

[60] J. John, A. P. Deshpande, and S. Varughese, "Morphology control and ionic crosslinking of pectin domains to enhance the toughness of solvent cast PVA/pectin blends," *Journal of Applied Polymer Science*, vol. 138, p. 50360, 2021, doi: 10.1002/app.50360.

[61] N. S. Said, I. F. Olawuyi, and W. Y. Lee, "Pectin hydrogels: Gel-forming behaviors, mechanisms, and food applications," *Gels*, vol. 9, p. 732, 2023, doi: 10.3390/gels9090732.

[62] M. Michael, M. Masytha, I. Iriany, and T. Taslim, "Multistage pectin extraction from lemon (*Citrus limon*) peel: Effect of nitric acid solvent pH and number of stages," *IOP Conference Series: Earth and Environmental Science*, vol. 1445, 2025, doi: 10.1088/1755-1315/1445/1/012054.

[63] S. Samal and I. Blanco, "Investigation of dispersion, interfacial adhesion of isotropic and anisotropic filler in polymer composite," *Applied Sciences*, vol. 11, no. 8, p. 8561, 2021, doi: 10.3390/app11188561.

[64] T. Huang, Y. Qin, M. Li, S. Gaol, and C. Shen, "Preparation and characterization of deacetylated konjac glucomannan/pectin composite films crosslinked with calcium hydroxide," *Journal of*

*Polymer Research*, vol. 29, p. 238, 2022, doi: 10.1007/s10965-022-03090-7.

[65] R. Sidabutar et al., "Synergistic integration of zeolite engineering and fixed-bed column design for enhanced biogas upgrading: Adsorbent synthesis, $CO_2/CH_4$ separation kinetics, and regeneration assessment," *Separation and Purification Technology*, vol. 355, p. 129722, 2025, doi: 10.1016/j.seppur.2024.129772.

[66] A. Mahmood et al., "Aloe vera-based polymeric network: A promising approach for sustained drug delivery, development, characterization, and *in vitro* evaluation," *Gels*, vol. 9, p. 474, 2023, doi: 10.3390/gels9060474.

[67] D. Sharma and B. Singh, "Designing aloe vera-sterculia gum based copolymeric hydrogel dressings for drug delivery," *Hybrid Advances*, vol. 5, 2024, doi: 10.1016/j.hybadv.2024.100142.

[68] N. S. Said, I. F. Olawuyi, and W. Y. Lee, "Pectin hydrogels: Gel-forming behaviors, mechanisms, and food applications," *Gels*, vol. 9, pp. 732, 2023, doi: 10.3390%2Fgels9090732.

[69] S. Zhao et al., "Elucidating the impact of intermolecular forces on the formation and internal structure of high-methoxyl pectin aggregates," *Food Chemistry*, vol. 487, 2025, p. 144765, doi: 10.1016/j.foodchem. 2025.144765.

[70] A. Kocira, K. Kozlowicz, K. Panasiewicz, M. Staniak, E. S. Krok, and P. Hortynska, "Polysaccharides as edible films and coatings: characteristics and influence on fruit and vegetable quality—A review," *Agronomy*, vol. 11, p. 813, 2021, doi: 10.3390/agronomy11050813.

[71] B. Surekha, P. Misra, A. C. Thippaiah, B. R. Shamanna, A. Madathilc, and M. Rajadurai, "A microneedle transdermal patch loaded with iron(II) nanoparticles for non-invasive sustained delivery to combat anemia," *Materials Advances*, vol. 5, pp. 3247–3256, 2024, doi: 10.1039/d3ma 01166f.

[72] A. Virani, V. Puri, H. Mohd, and B. Michniak-Kohn, "Effect of penetration enhancers on transdermal delivery of oxcarbazepine, an antiepileptic drug using microemulsions," *Pharmaceutics*, vol. 15, p. 183, 2023, doi: 10.3390/pharmaceutics15010183.

[73] R. K. Arya, D. Thapliyal, J. Sharma, and G. D. Verros, "Glassy polymers—Diffusion, sorption, ageing and applications," *Coatings*, vol. 11, p. 1049, 2021, doi: 10.3390/coatings11091049.

[74] R. T. Stiepel et al., "A predictive mechanistic model of drug release from surface eroding polymeric nanoparticles," *Journal of Controlled Release*, vol. 351, pp. 883–895, 2022, doi: 10.1016/j.jconrel.2022.09.067.

[75] A. K. Kodoth, V. M. Ghate, S. A. Lewis, B. Prakash, and V. Badalamoole, "Pectin-based silver nanocomposite film for transdermal delivery of Donepezil," *International Journal of Biological Macromolecules*, vol. 134, pp. 269–279, 2019, doi: 10.1016/j.ijbiomac.2019.04.191.

[76] Z. Li, M. Cai, K. Yang, and P. Sun, "Kinetic study of d-limonene release from finger citron essential oil loaded nanoemulsions during simulated digestion in vitro," *Journal of Functional Foods*, vol. 58, pp. 67–73, 2019, doi: 10.1016/j.jff.2019.04.056.

[77] M. Ganje, S. M. Jafari, A. M. Tamadon, M. Niakosari, and Y. Maghsoudlou, "Mathematical and fuzzy modeling of limonene release from amylose nanostructures and evaluation of its release kinetics," *Food Hydrocolloids*, vol. 95, pp. 186–194, 2019, doi: 10.1016/j.foodhyd.2019. 04.039.

[78] D. Yan, W. Ouyang, J. Lin, and Z. Liu, "Smart coating by thermo-sensitive Pluronic F-127 for enhanced corneal healing via delivery of biological macromolecule progranulin," *International Journal of Biological Macromolecules*, vol. 253, p. 127586, 2023, doi: 10.1016/j.ijbiomac.2023. 127586.

[79] E. M. Eissa et al., "pH-Sensitive in situ gel of mirtazapine invasomes for rectal drug delivery: protruded bioavailability and anti-depressant efficacy," *Pharmaceuticals*, vol. 17, p. 978, 202, doi: 10.3390/ph17080978.